Supplementary Information

Comprehensive Design, Synthesis of Methyl Substituted Benzimidazole-based Mononuclear Copper(II) Complexes and Evaluation of DNA Cleavage and ROS-induced Apoptosis

Manoj Kumar Kumawat[a], Shobhit Mathur[a], Sharan Shanmuga Vuppaladadium Rathnam[b], Jitender Jangra [b], Roy Anindya[b], Somnath Maji[a]*

[a]Department of Chemistry, Indian Institute of Technology Hyderabad, Kandi, Sangareddy 502284, Telangana, India

[b]DNA Repair Research Lab, Department of Biotechnology, Indian Institute of Technology Hyderabad, Kandi, Sangareddy 502284, Telangana, India

*Corresponding author

Email address: smaji@chy.iith.ac.in (Somnath Maji).

Table S1 IR vibrational frequencies (cm^{-1}) of compound

Compound	νClO_4^-	$\nu C=N$	$\nu C-N$	$\nu =C-H$
L	–	1473	1332	740
1	1083/624	1491	1307	752
2	1085/624	1507	1316	757
3	1080/621	1496	1329	755
4	1084/624	1490	1326	751

Table S2 Selected crystallographic data for complexes 1–4

Complex	**1**	**2**	**3**	**4**
Empirical formula	$C_{30}H_{30.8}Cl_2CuN_8O_{8.4}$	$C_{34}H_{33}Cl_2CuN_9O_8$	$C_{32}H_{31}Cl_2CuN_7O_8$	$C_{32}H_{27}Cl_2CuN_9O_8$
Formula weight	772.26	830.148	776.096	800.06
Temperature/K	298.00	298.00	172.00	273.15
Crystal system	triclinic	orthorhombic	monoclinic	triclinic
Space group	*P*-1	*Pnma*	$P2_1$	*P*-1
a/Å	12.3764(10)	10.7413(7)	8.2663(7)	10.3672(9)
b/Å	12.7856(12)	11.3260(7)	20.2627(18)	11.7373(12)
c/Å	13.4518(12)	30.914(2)	10.2878(10)	13.8620(14)
α/°	95.205(3)	90	90	83.732(4)
β/°	115.840(3)	90	93.252(3)	88.201(3)
γ/°	111.233(3)	90	90	86.873(3)
Volume/Å^3	1705.5(3)	3760.9(4)	1720.4(3)	1673.6(3)
Z	2	4	2	2
ρ_{calc}g/cm^3	1.504	1.466	1.498	1.588
μ/mm^{-1}	0.860	0.785	0.851	0.879
F(000)	794.0	1711.7	799.8	818.0
Crystal size/mm^3	0.15 × 0.08 × 0.06	0.08 × 0.05 × 0.04	0.07 × 0.05 × 0.04	0.12 × 0.08 × 0.06
Radiation	MoKα (λ = 0.71073)	MoKα (λ = 0.71073)	Mo Kα (λ = 0.71073)	MoKα (λ = 0.71073)
2θ range for data collection/°	3.82 to 54.32	4.02 to 54.26	4.02 to 54.3	3.936 to 54.404

Index ranges	$-15 \le h \le 15$, $-16 \le k \le 16$, $-17 \le l \le 17$	$-13 \le h \le 13$, $-14 \le k \le 14$, $-39 \le l \le 39$	$-10 \le h \le 9$, $-25 \le k \le 25$, $-12 \le l \le 13$	$-13 \le h \le 12$, $-15 \le k \le 15$, $-17 \le l \le 17$
Reflections collected	41144	49292	15979	38425
Independent reflections	7552 [R_{int} = 0.0549, R_{sigma} = 0.0370]	4369 [R_{int} = 0.1059, R_{sigma} = 0.0494]	7030 [R_{int} = 0.0387, R_{sigma} = 0.0556]	7424 [R_{int} = 0.0692, R_{sigma} = 0.0551]
Data/restraints/parameters	7551/144/529	4369/0/249	7030/19/466	7424/0/475
Goodness-of-fit on F^2	1.028	1.045	1.025	1.016
Final R indexes [I>=2σ (I)]	R_1 = 0.0406, wR_2 = 0.1118	R_1 = 0.0654, wR_2 = 0.1855	R_1 = 0.0495, wR_2 = 0.1295	R_1 = 0.0511, wR_2 = 0.1245
Final R indexes [all data]	R_1 = 0.0503, wR_2 = 0.1191	R_1 = 0.1096, wR_2 = 0.2205	R_1 = 0.0589, wR_2 = 0.1371	R_1 = 0.0859, wR_2 = 0.1434
Largest diff. peak/hole / e Å^{-3}	0.48/-0.34	0.85/-1.02	0.54/-0.39	0.65/-0.55

Table S3 Selected bond lengths (Å) and bond angles (°)

Complex 1					
Cu1–N1	2.332(2)	Cu1–N2	2.0032(17)	Cu1–N3	1.9922(18)
Cu1–N4	2.0091(18)	Cu1–N5	2.0107(18)	Cu1–O8	2.596(6)
N1–Cu1–N2	78.80(7)	N1–Cu1–N3	80.07(7)	N1–Cu1–N4	101.55(7)
N1–Cu1–N5	99.98(7)	N2–Cu1–N3	88.46(7)	N2–Cu1–N4	96.48(7)
N2–Cu1–N5	176.84(7)	N3–Cu1–N4	175.01(7)	N3–Cu1–N5	94.22(7)
N4–Cu1–N5	80.87(7)	N1–Cu1– O8	172.47(15)	N2–Cu1–O8	93.75(15)
N3–Cu1– O8	98.84(16)	N4–Cu1– O8	80.17(16)	N5–Cu1– O8	87.51(15)

Complex 2					
Cu1–N1	2.348(5)	Cu1–N2	1.985(4)	Cu1–N2$^{/}$	1.985(4)
Cu1–N4	2.017(4)	Cu1–N4$^{/}$	2.017(4)	Cu1–O1	2.730
N1–Cu1– N2	78.97(14)	N1–Cu1–N2$^{/}$	78.97(14)	N1–Cu1–N4	102.12(13)
N1–Cu1– N4$^{/}$	102.12(13)	N2–Cu1–N4	175.54(15)	N2–Cu1–N4$^{/}$	93.89(15)
N2–Cu1– N2$^{/}$	90.6(2)	N2$^{/}$–Cu1–N4	93.89(15)	N2$^{/}$–Cu1– N4$^{/}$	175.54(15)
N4–Cu1– N4$^{/}$	81.7(2)	N1–Cu1– O1	175.29	N2–Cu1–O1	97.77
N2$^{/}$–Cu1– O1	97.77	N4–Cu1– O1	81.39	N4$^{/}$–Cu1– O1	81.39

Complex 3					
Cu1–N1	2.109(8)	Cu1–N2	1.976(3)	Cu1–N3	1.981(3)
Cu1–N4	2.113(3)	Cu1–N5	2.130(3)	Cu1–N8	2.087(5)
N1–Cu1–N2	81.1(2)	N1–Cu1–N3	80.9(2)	N1–Cu1–N4	155.6(2)
N1–Cu1–N5	125.3(2)	N1–Cu1–N8	26.8(2)	N2–Cu1–N3	161.66(12)
N2–Cu1–N4	96.73(13)	N2–Cu1–N5	97.17(12)	N2–Cu1–N8	80.77(17)
N3–Cu1–N4	98.18(13)	N3–Cu1–N5	96.08(12)	N3–Cu1–N8	81.57(17)
N4–Cu1–N5	79.12(13)	N4–Cu1–N8	128.81(18)	N5–Cu1–N8	152.07(18)

Complex 4					
Cu1–N1	2.342(3)	Cu1–N2	2.004(3)	Cu1–N3	2.003(3)
Cu1–N4	2.007(3)	Cu1–N5	2.051(3)	Cu1–O1	2.549
N1–Cu1–N2	79.35(11)	N1–Cu1–N3	78.46(11)	N1–Cu1–N4	101.20(11)
N1–Cu1–N5	97.89(10)	N2–Cu1–N3	90.95(11)	N2–Cu1–N4	96.24(11)
N2–Cu1–N5	175.80(10)	N3–Cu1–N4	172.63(11)	N3–Cu1–N5	91.60(11)
N4–Cu1–N5	81.13(10)	N1–Cu1– O1	172.93	N2–Cu1–O1	99.47
N3–Cu1– O1	94.51	N4–Cu1– O1	85.95	N5–Cu1– O1	83.67

Table S4 EPR *g* values and redox potential data for complexes 1–4

Complex	**EPR data/*g* values**						**Redox data**		
	$g_{\parallel}$	$g_{\perp}$	$A_{\parallel}$[a]	$g_{\parallel}/A_{\parallel}$	**G**	α^2	**Cu(III)/ Cu(II)[b]**	**Cu(II)/ Cu(I)[b]**	**Ligand-based[b]**
1	2.211	2.048	159.7	138.4	4.4	0.71	0.132	–0.072	–1.612
2	2.207	2.053	159.3	138.5	3.9	0.71	0.144	–0.084	–1.528
3	2.185	2.042	184.4	118.5	4.4	0.75	0.634	–0.110	–1.428, –1.596
4	2.204	2.055	161.2	136.7	3.7	0.71	0.176	–0.076	–1.024, –1.328, –1.592

[a] $A_{\parallel} \times 10^{-4}$ cm^{-1}; [b] Potentials $E_{1/2}°_{298\,K}$ (V) *vs* SCE in dry DMF/0.1 M TBAP.

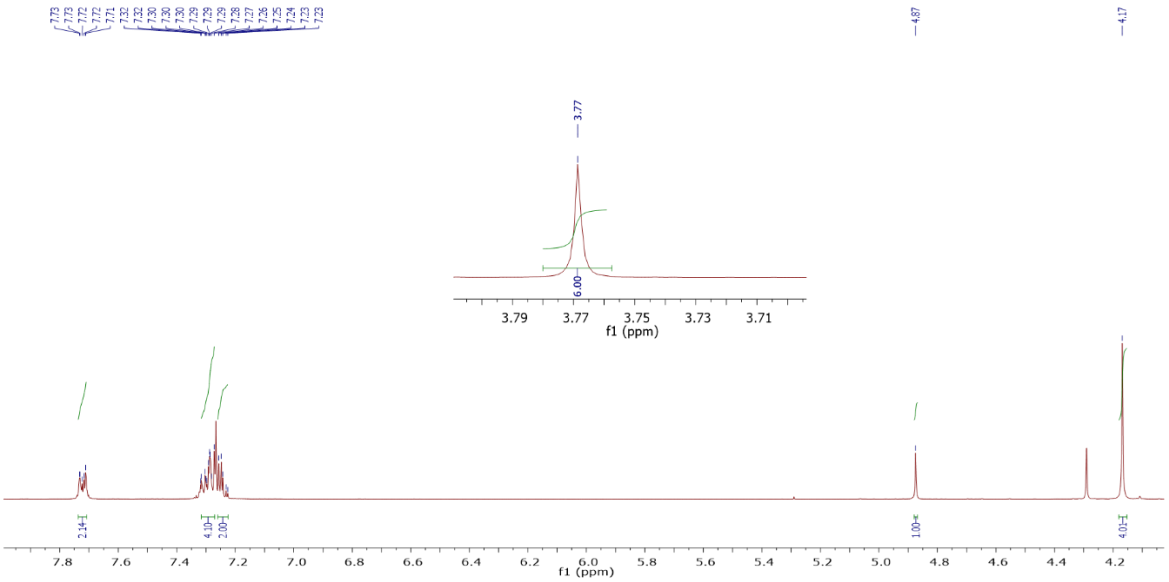

Fig. S1 ^{1}H NMR spectra of **L** in $CDCl_3$ at room temperature.

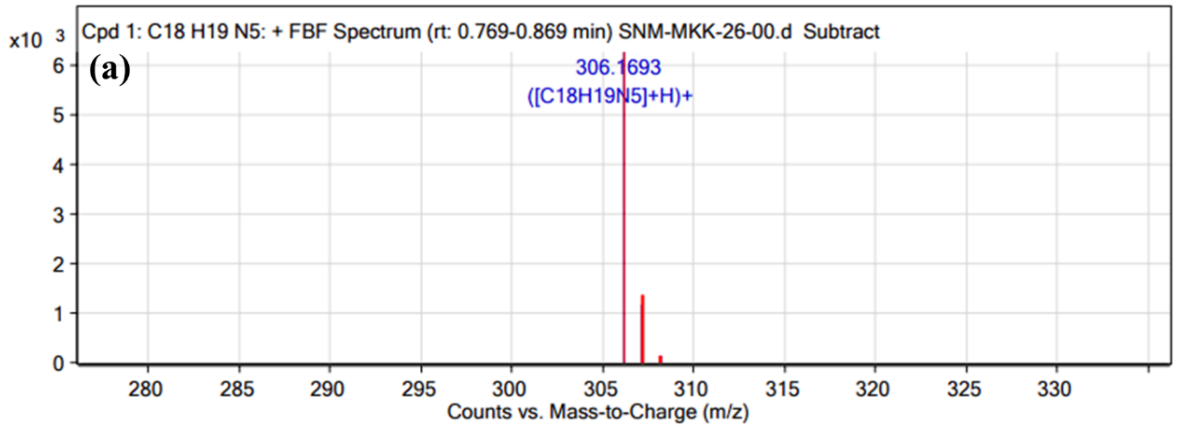

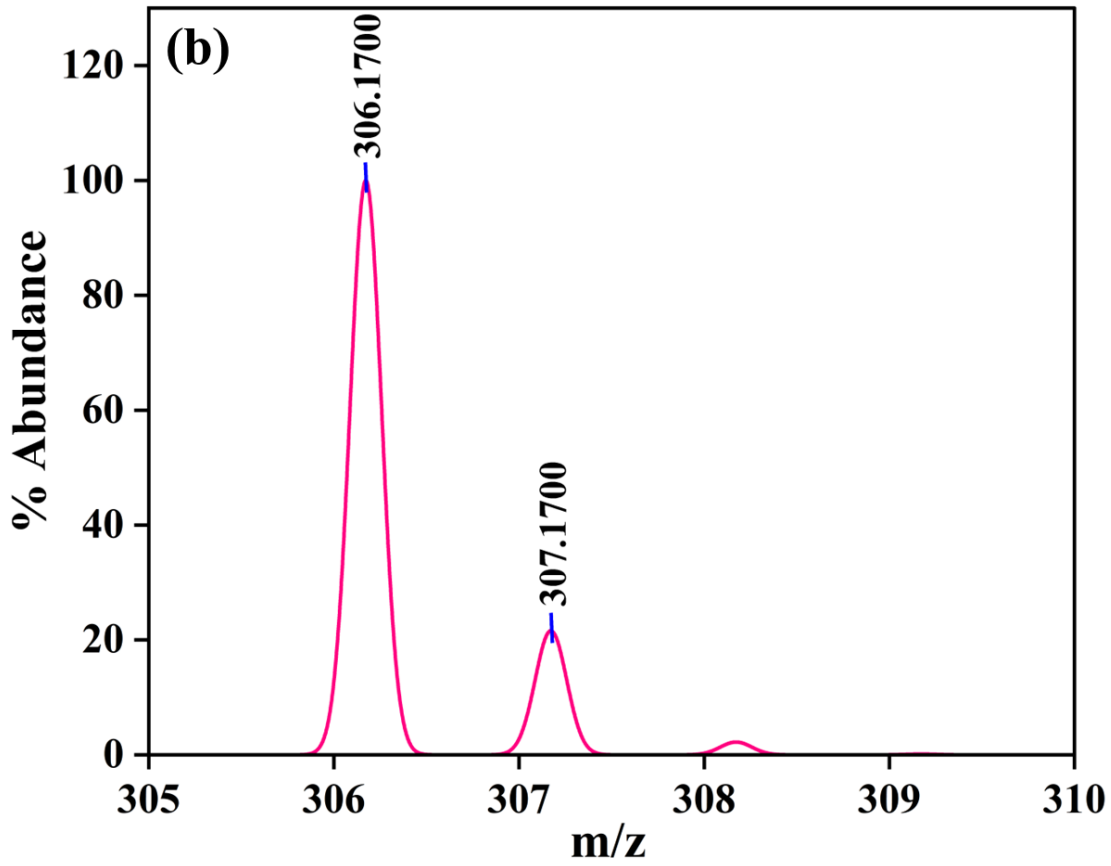

Fig. S2 HRMS spectra of the **L** (a) experimental, (b) simulated.

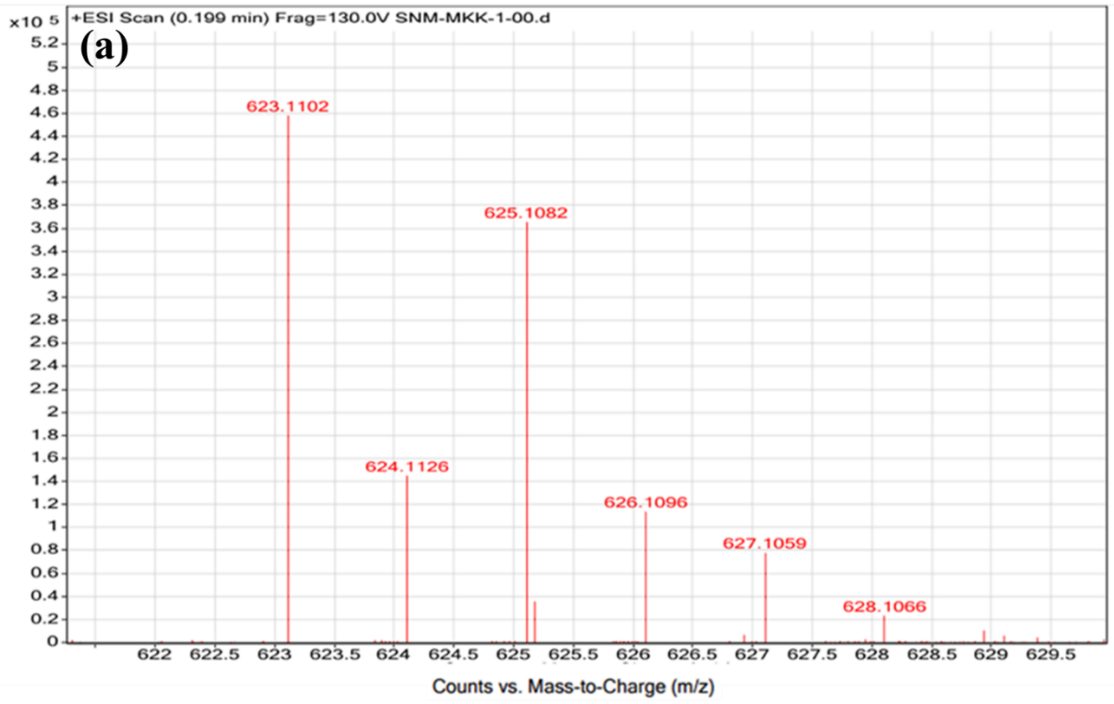

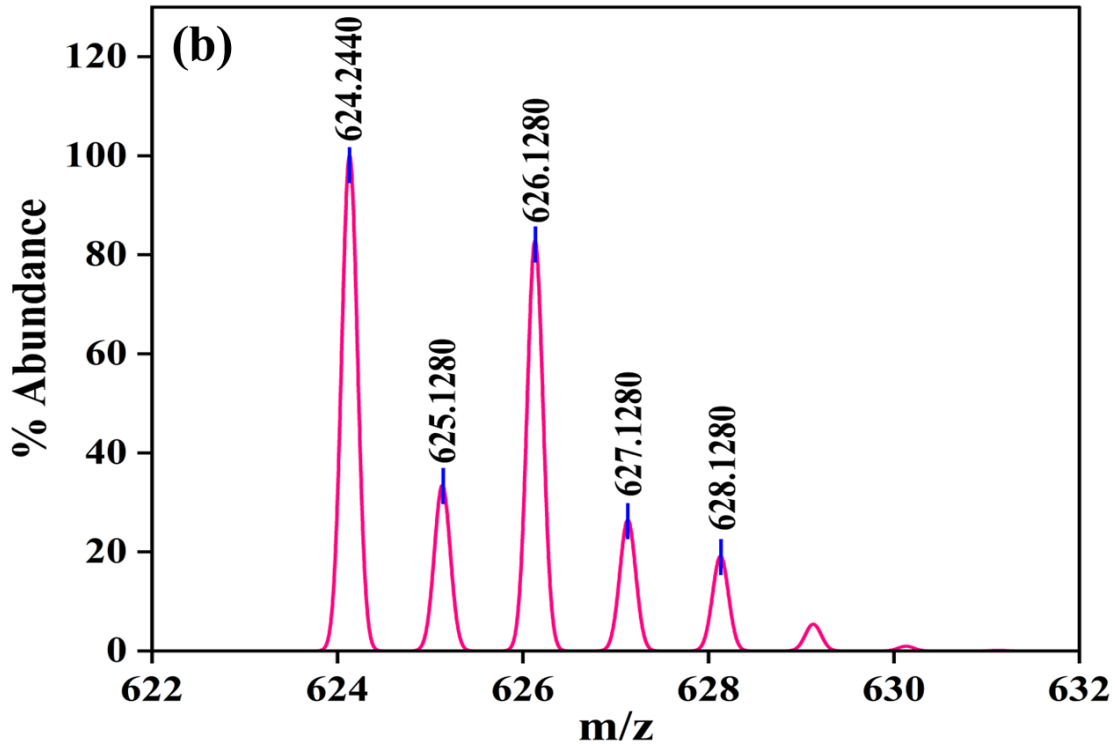

Fig. S3 HRMS spectra of the **1** (a) experimental, (b) simulated.

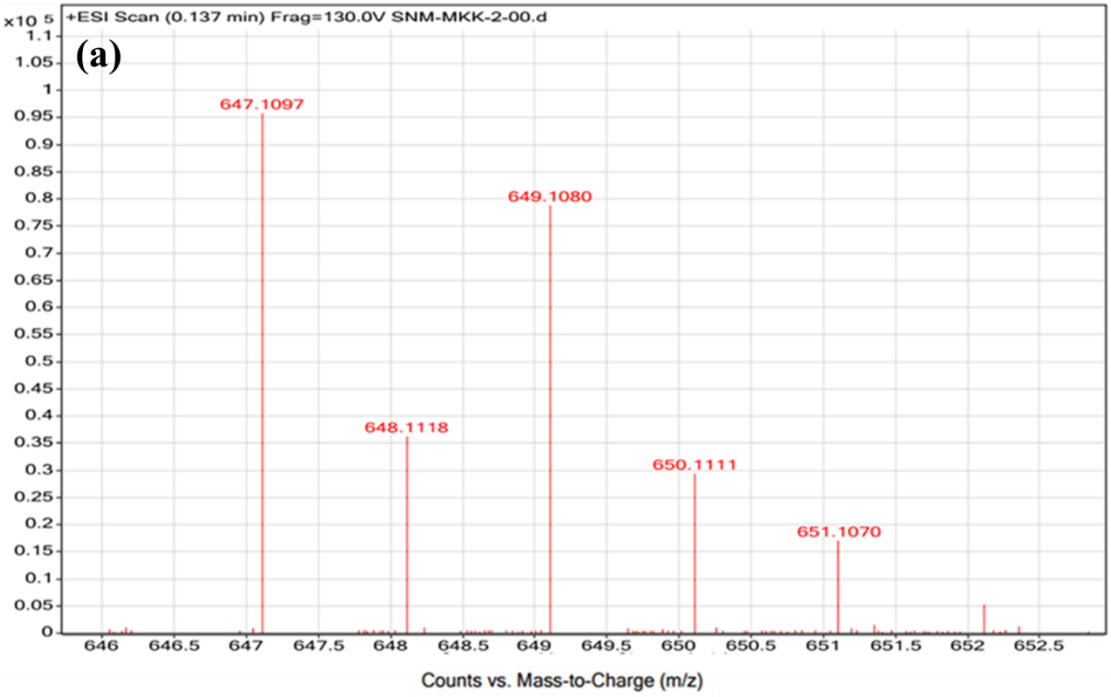

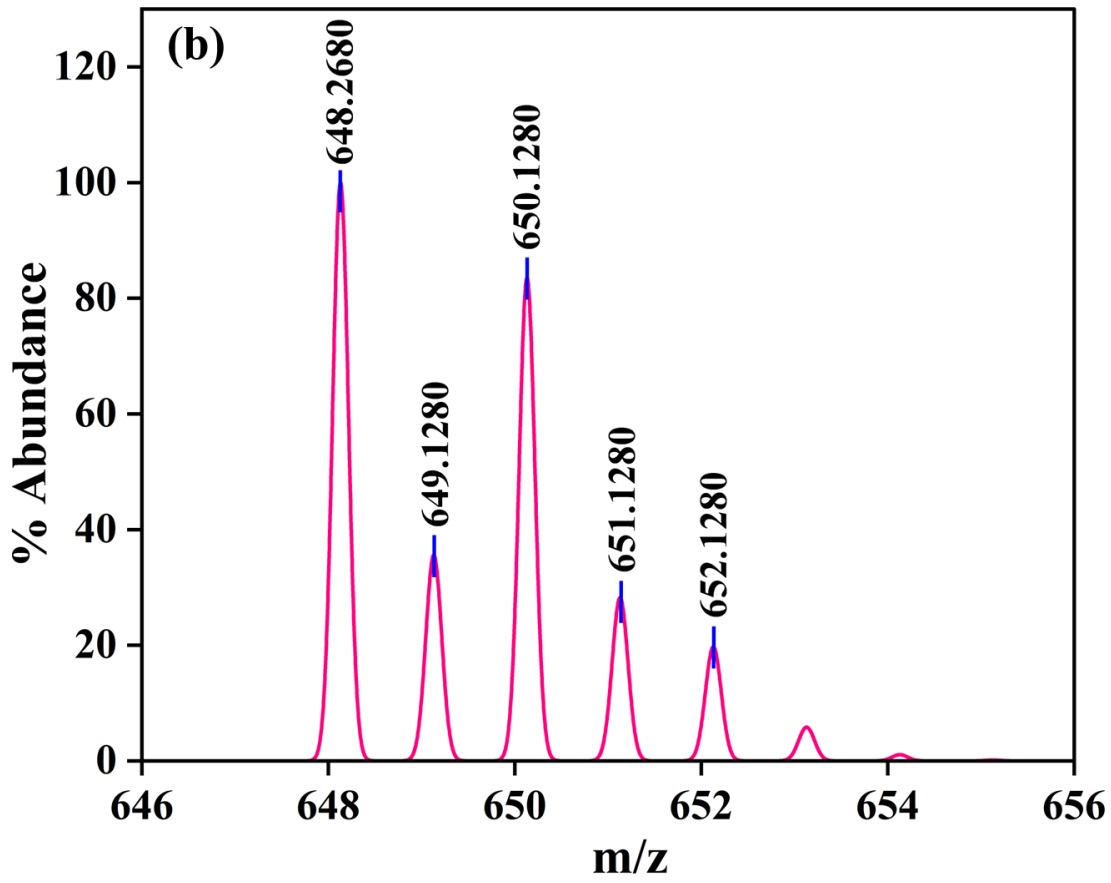

Fig. S4 HRMS spectra of the **2** (a) experimental, (b) simulated.

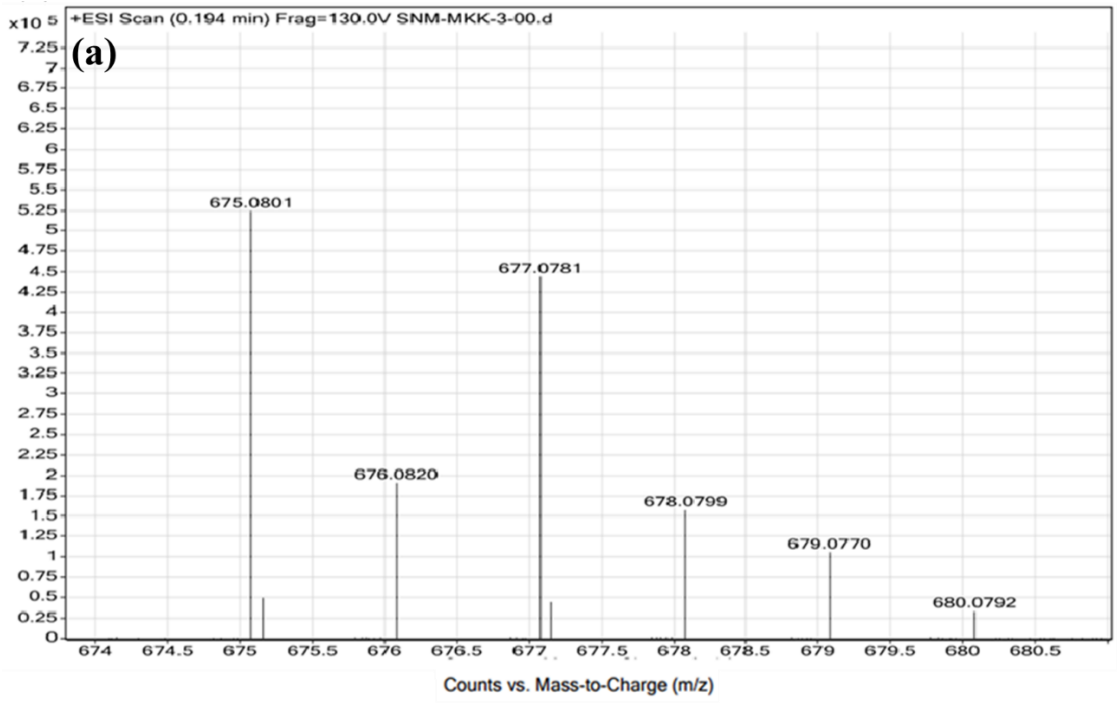

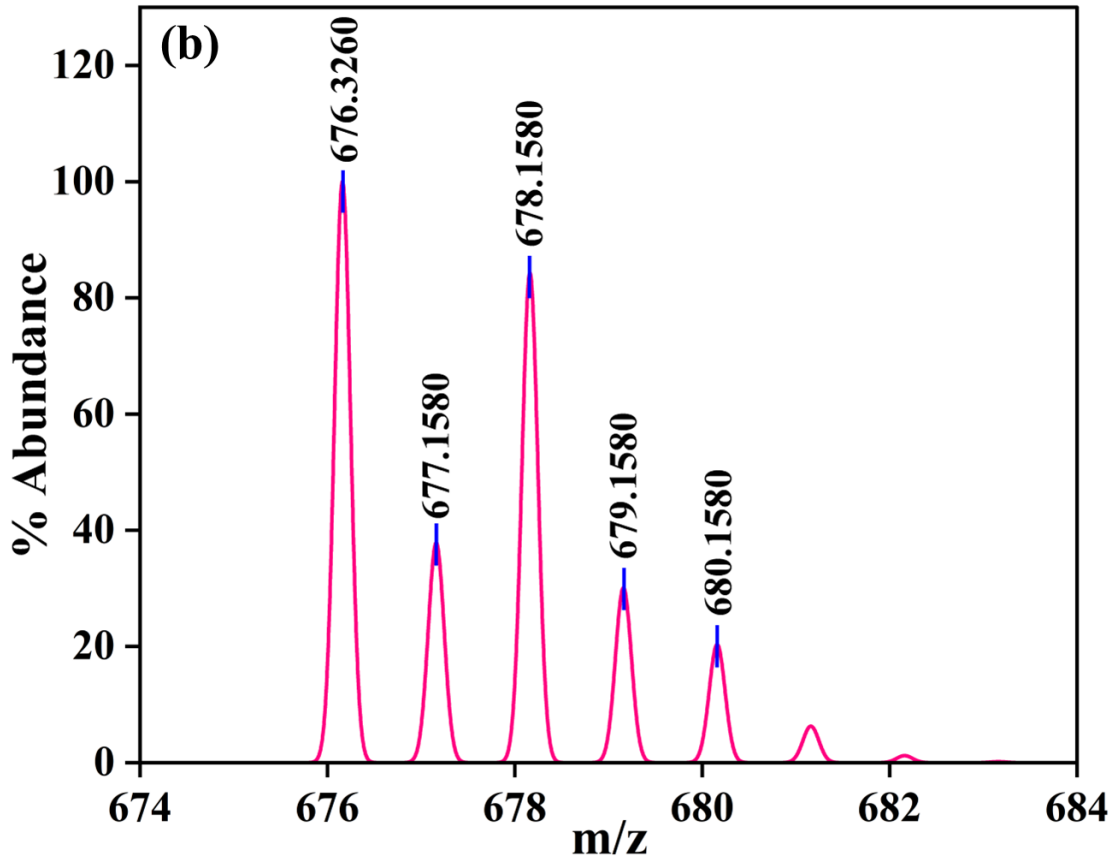

Fig. S5 HRMS spectra of the **3** (a) experimental, (b) simulated.

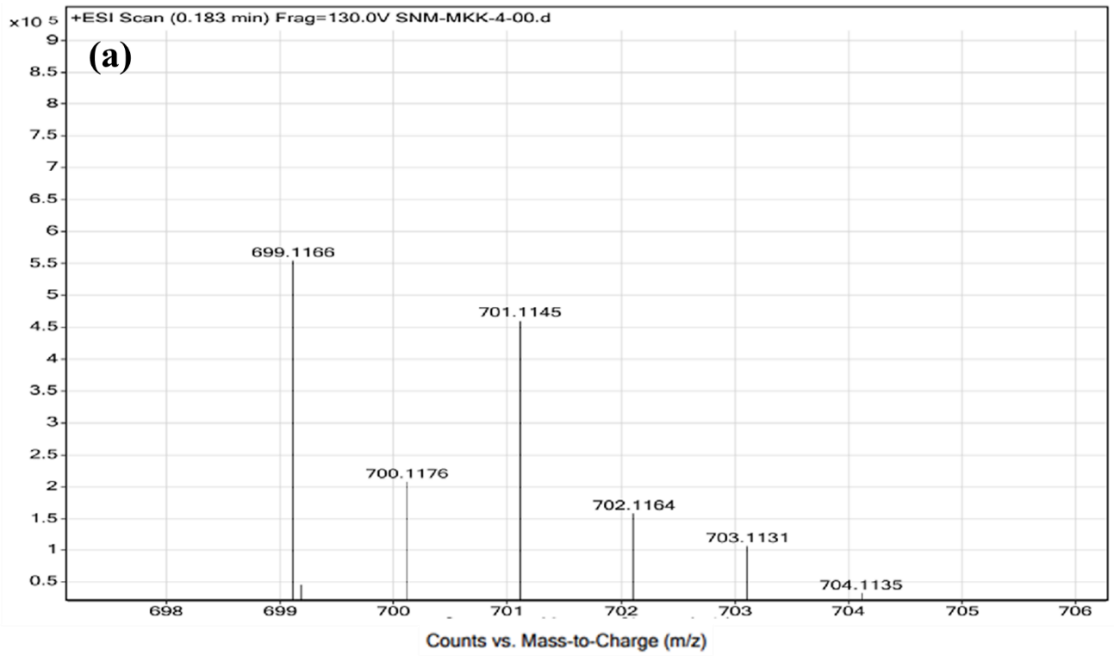

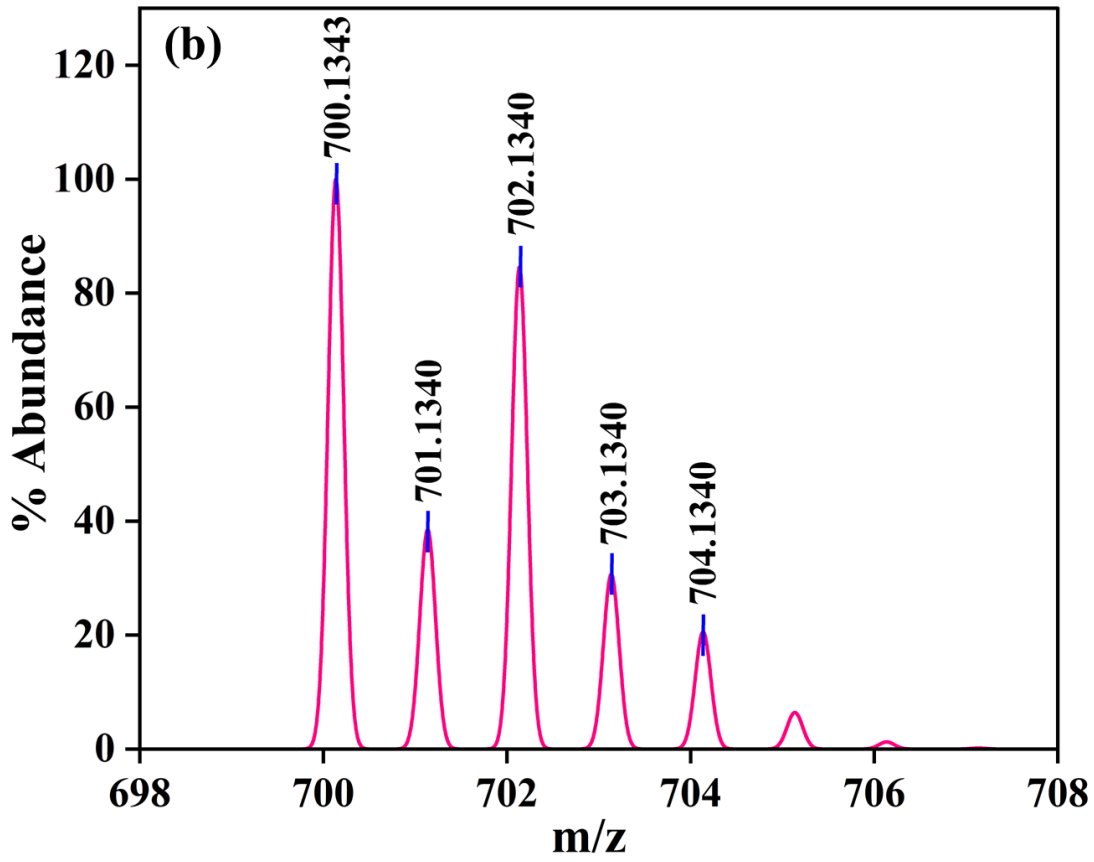

Fig. S6 HRMS spectra of the **4** (a) experimental, (b) simulated.

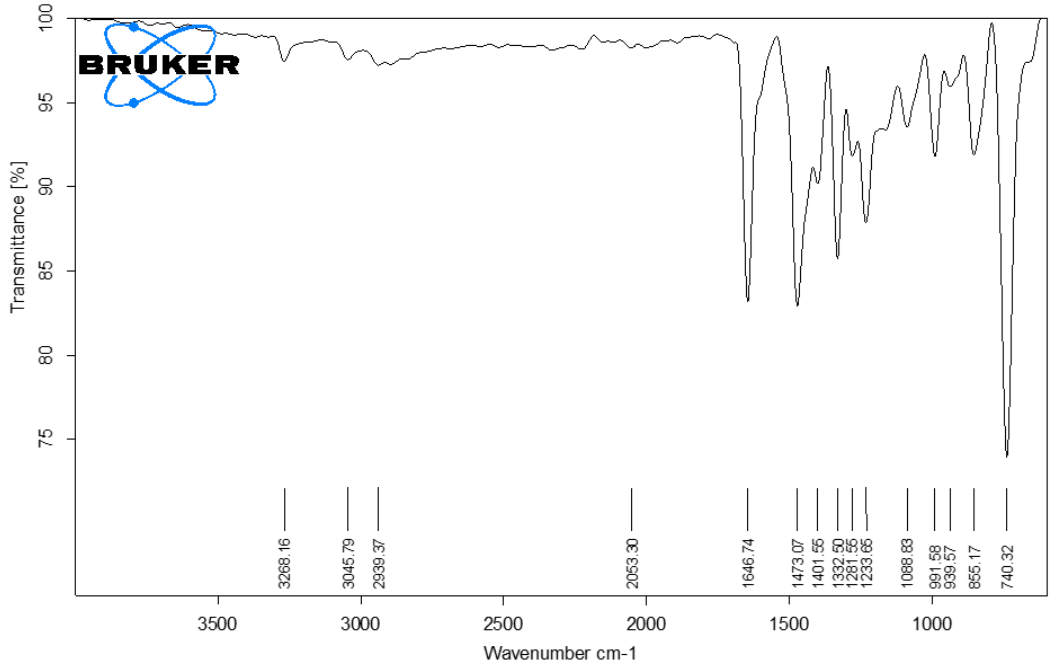

Fig. S7 FT-IR (solid) spectra of **L**.

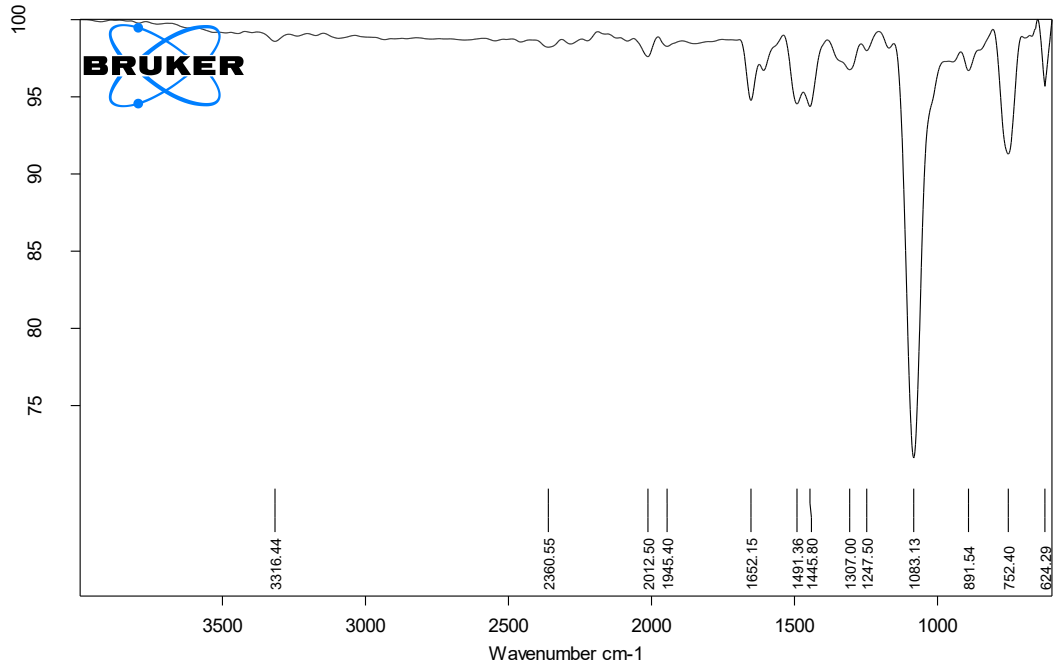

Fig. S8 FT-IR (solid) spectra of **1**.

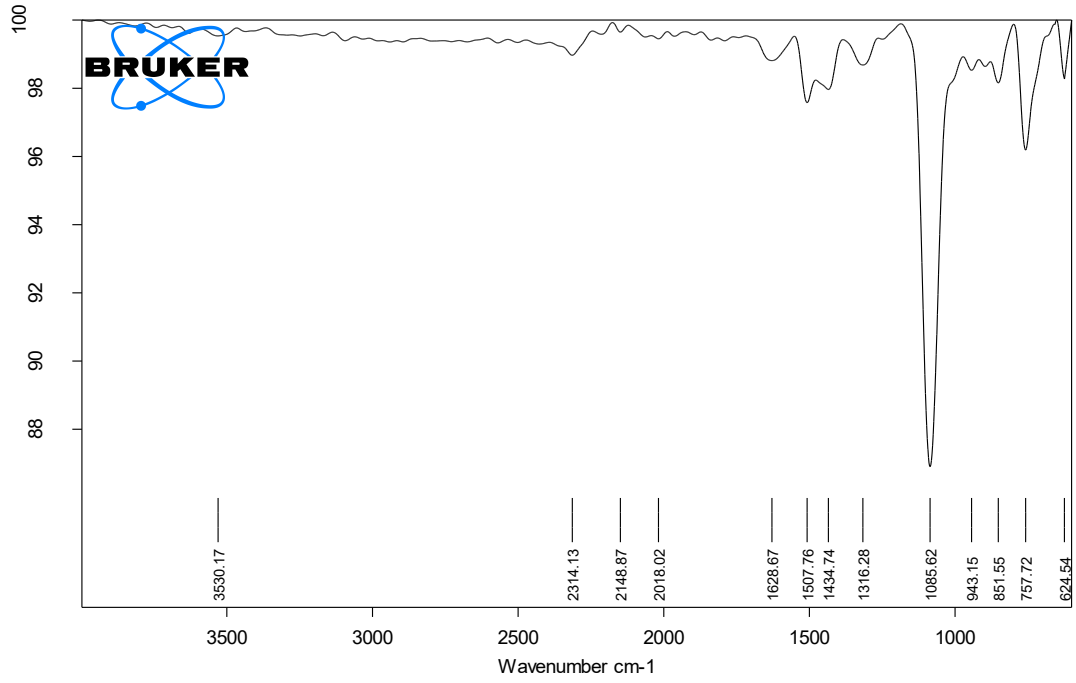

Fig. S9 FT-IR (solid) spectra of **2**.

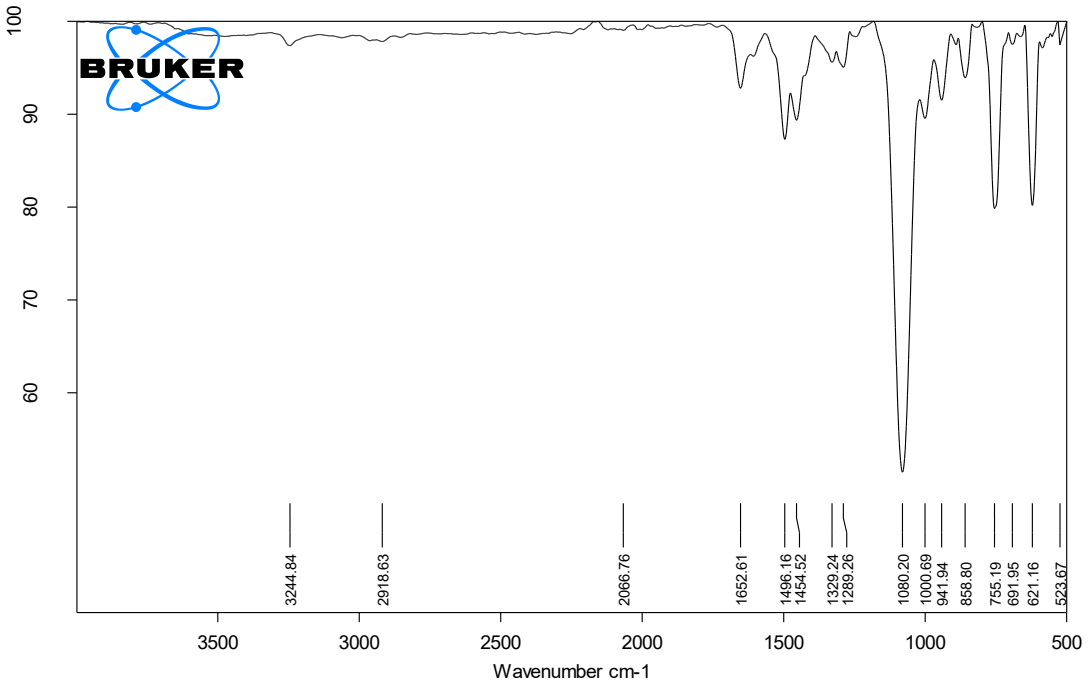

Fig. S10 FT-IR (solid) spectra of **3**.

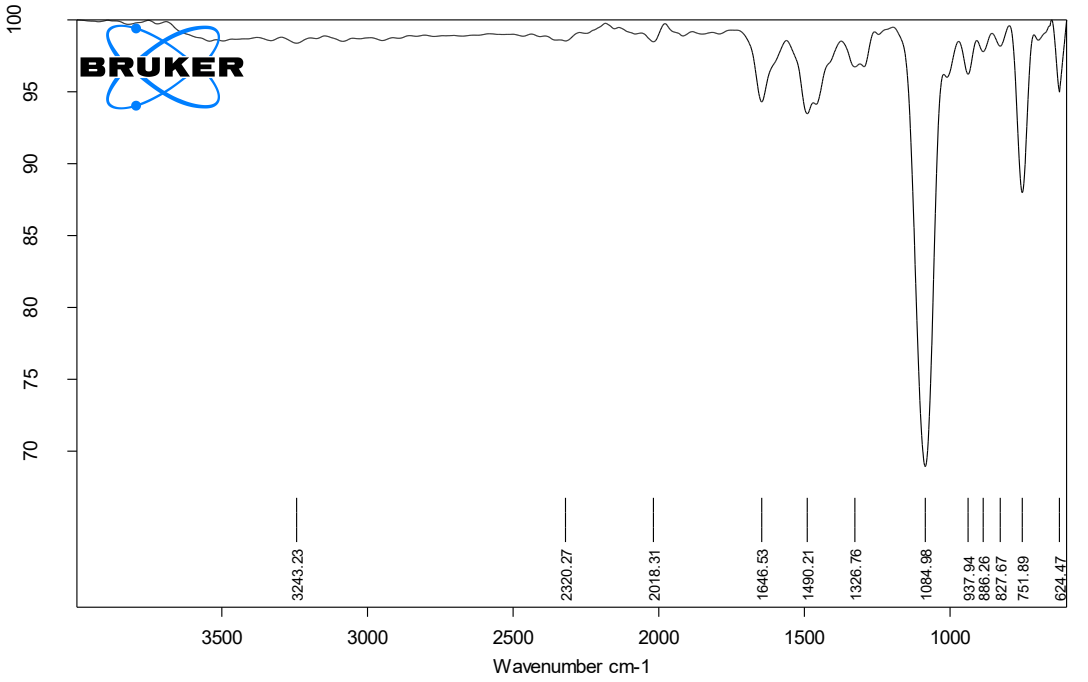

Fig. S11 FT-IR (solid) spectra of **4**.

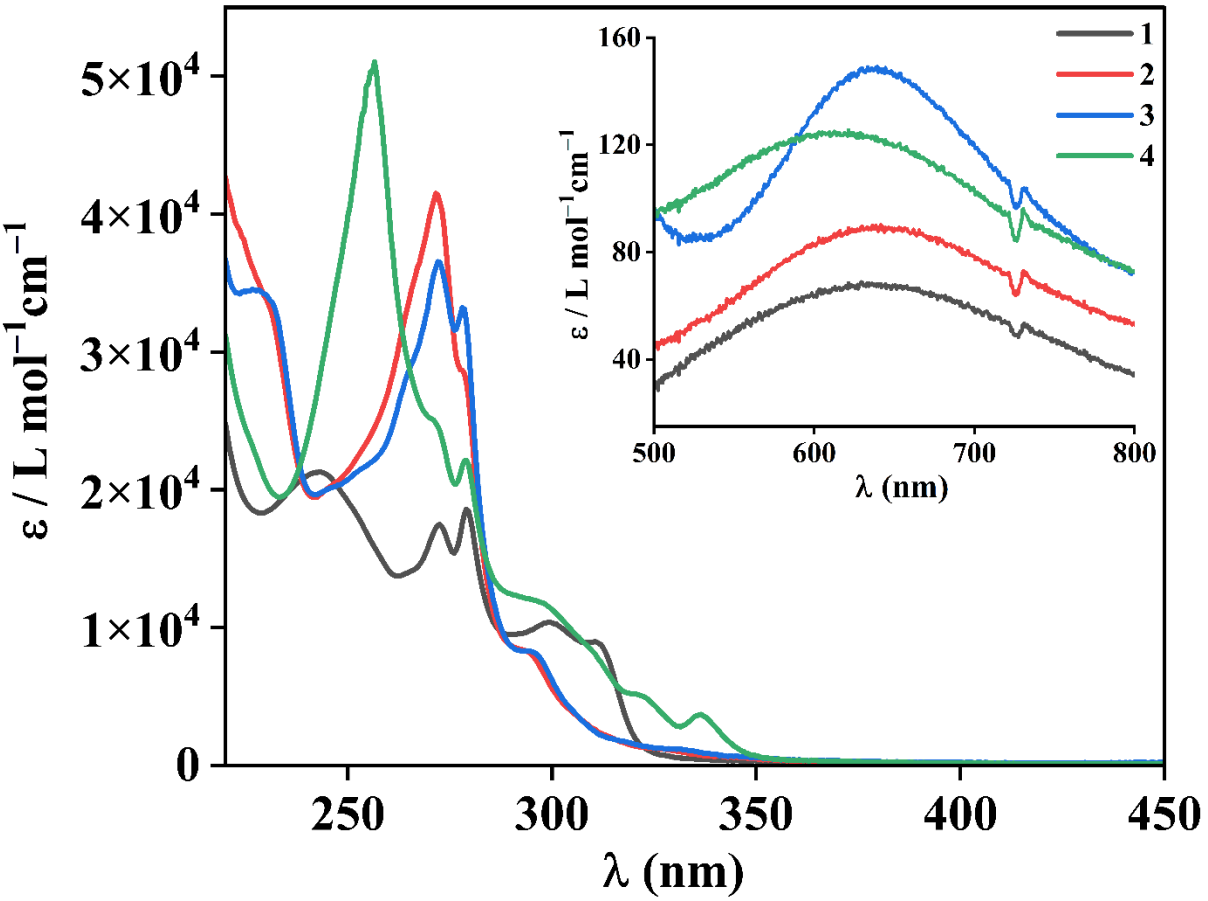

Fig. S12 The UV-vis spectra of **1–4** in 5 mM Tris-HCl buffer (pH 7.4) at room temperature.

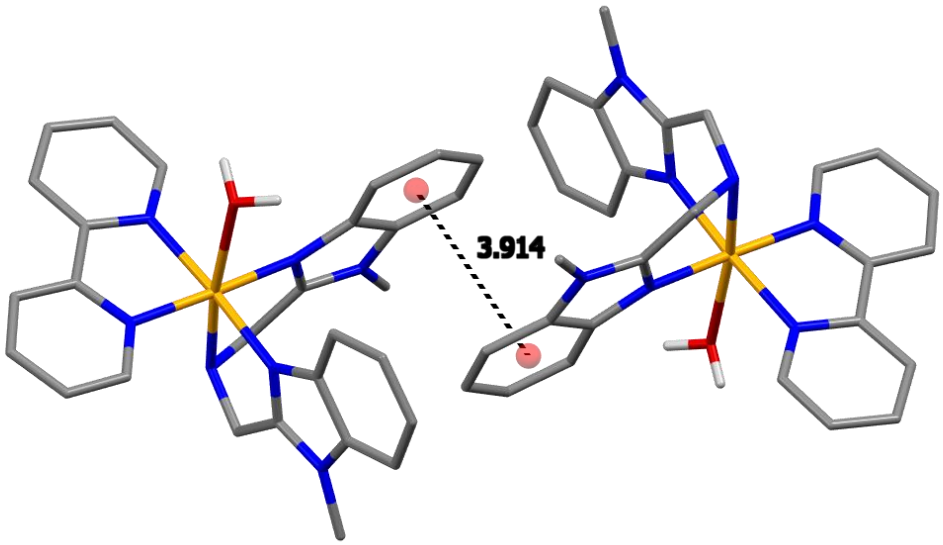

Fig. S13 Displaced π−π stacking present in the crystal symmetry of **1**.

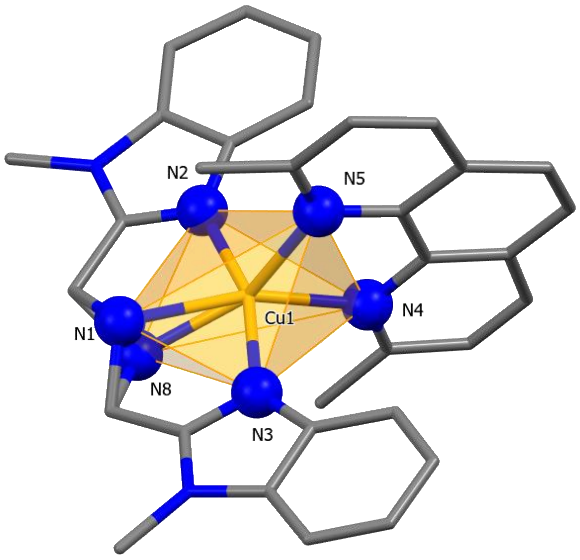

Fig. S14 The polyhedron view of the complex **3** around the Cu1 centre.

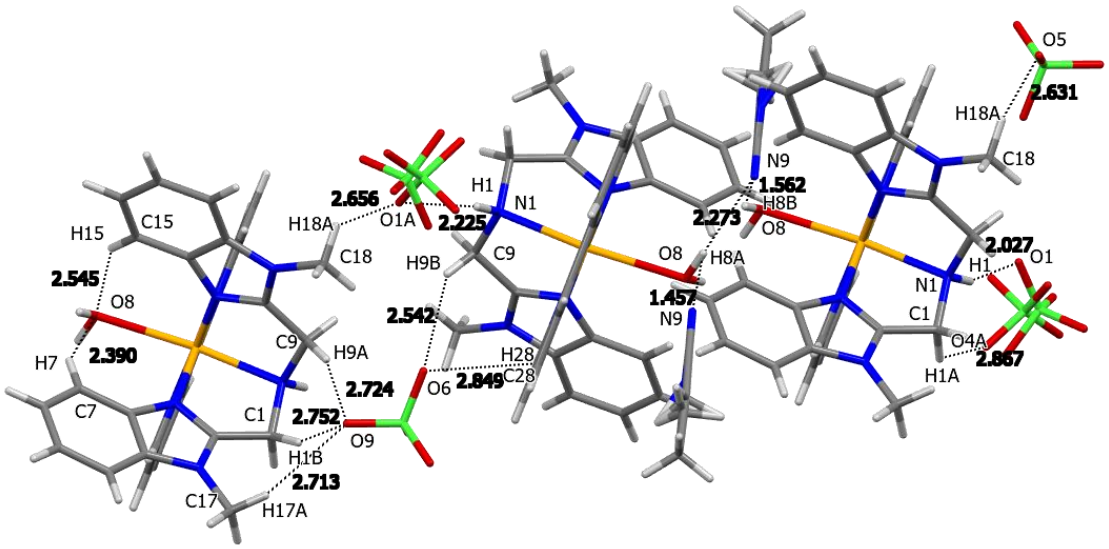

Fig. S15 Intermolecular H-bonding interactions present in the crystal symmetry of **1**.

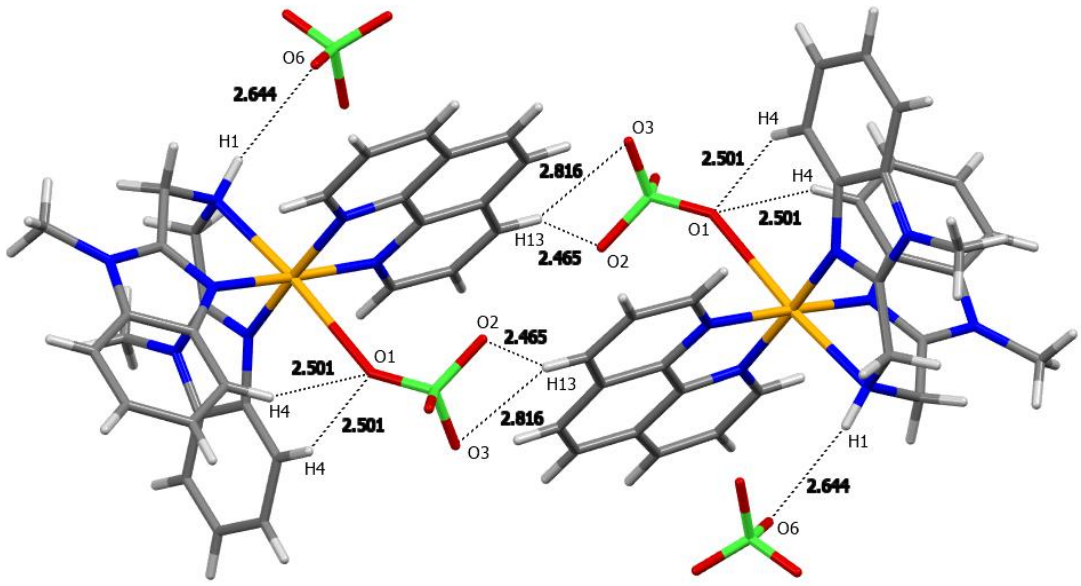

Fig. S16 Intermolecular H-bonding interactions present in the crystal symmetry of **2**.

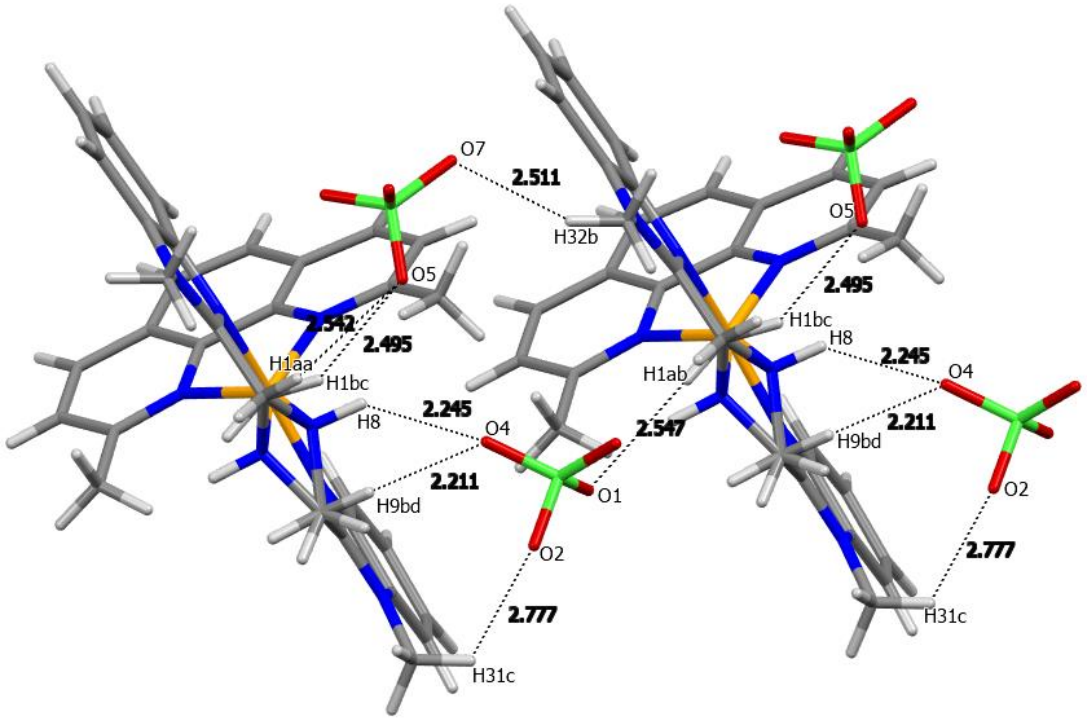

Fig. S17 Intermolecular H-bonding interactions present in the crystal symmetry of **3**.

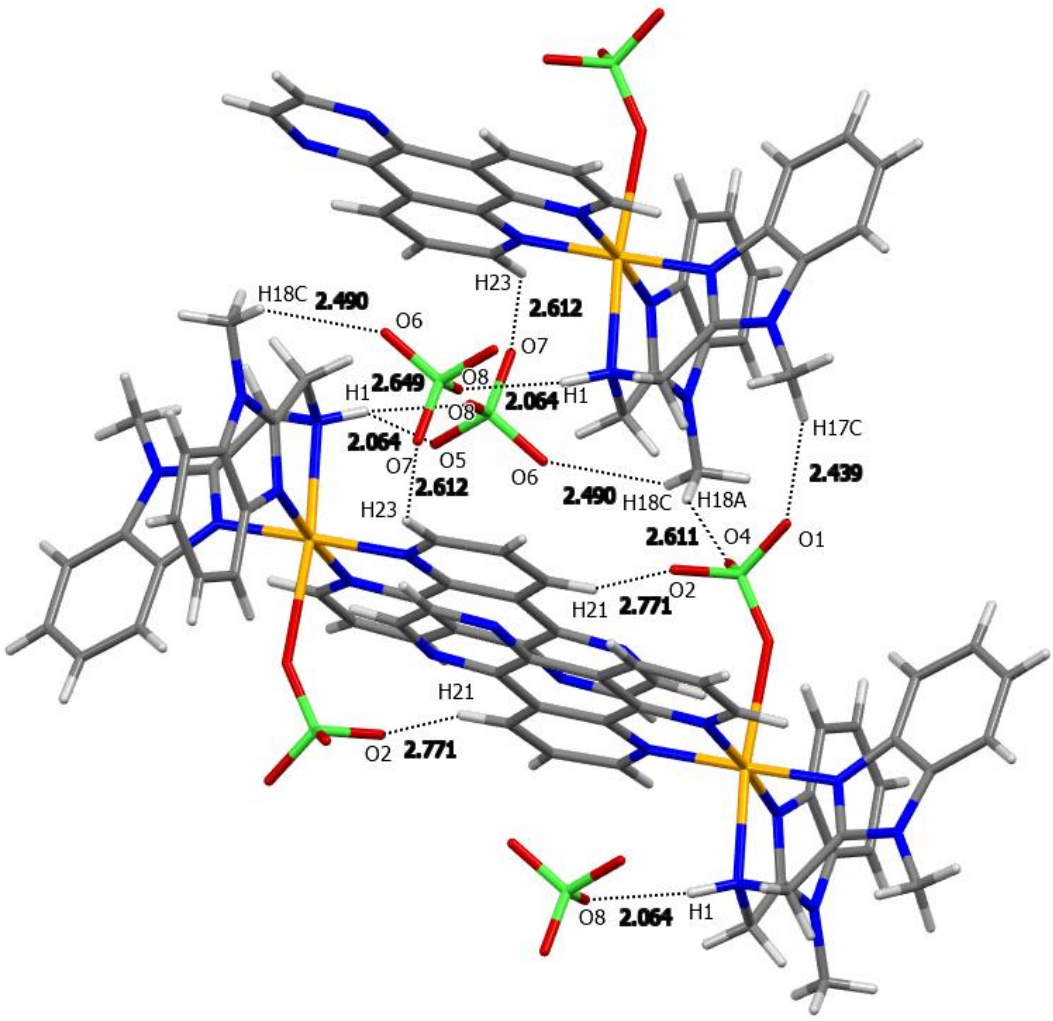

Fig. S18 Intermolecular H-bonding interactions present in the crystal symmetry of **4**.

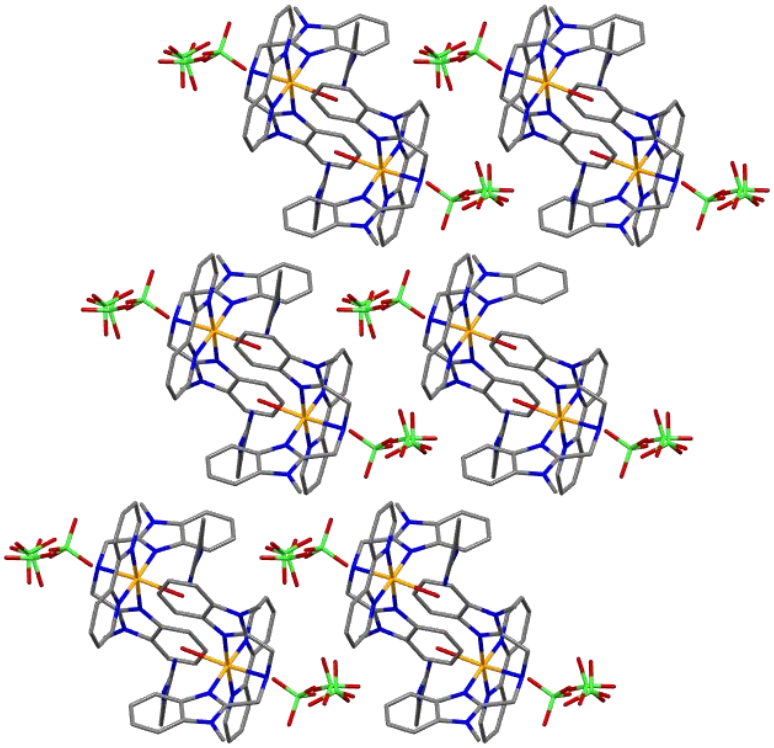

Fig. S19 Crystal packing of **1** viewed along the *a*-axis.

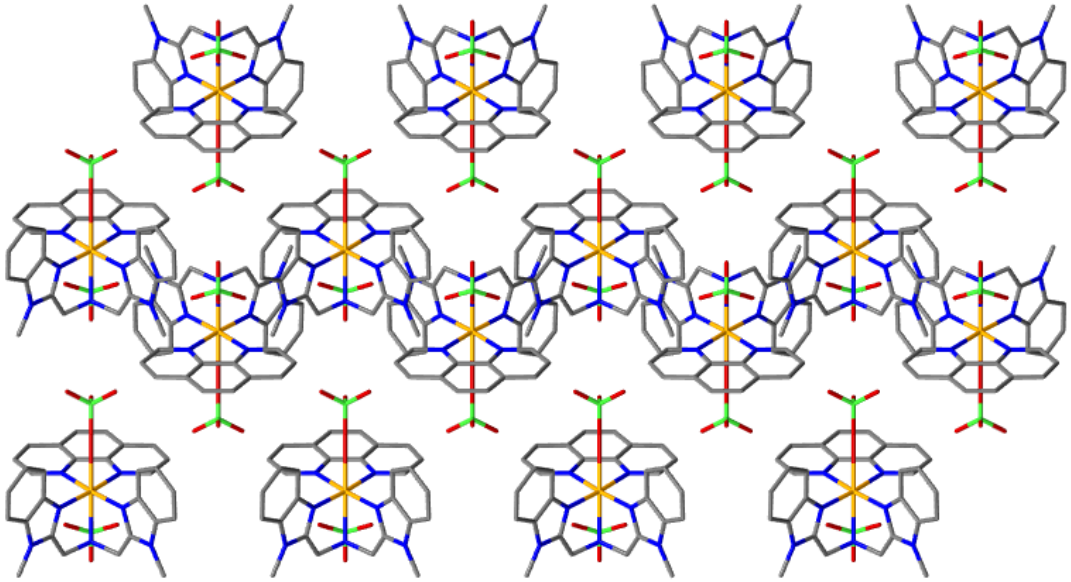

Fig. S20 Crystal packing of **2** viewed along the *a*-axis.

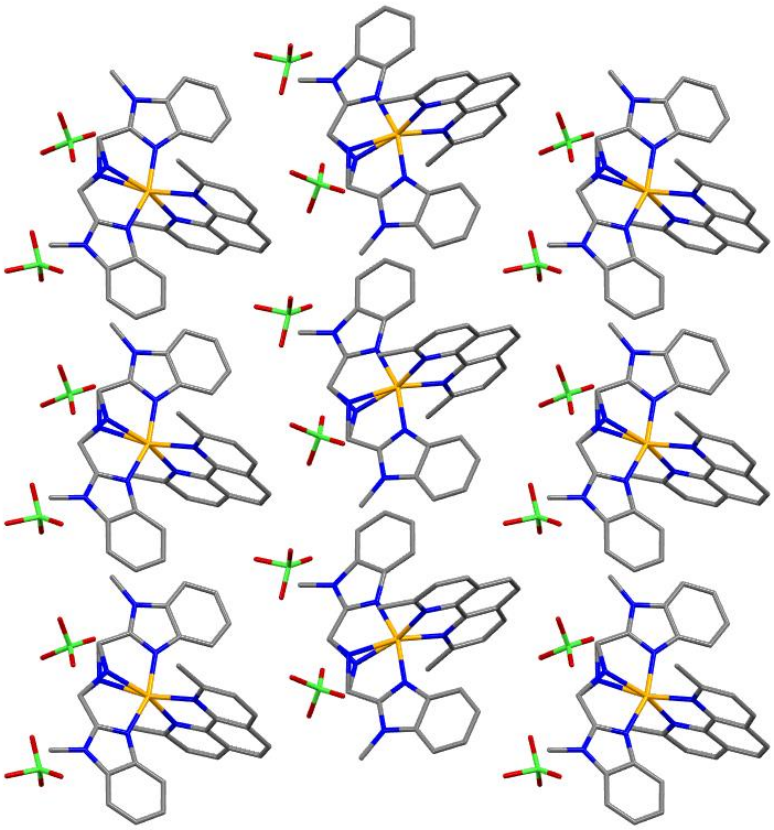

Fig. S21 Crystal packing of **3** viewed along the *a*-axis.

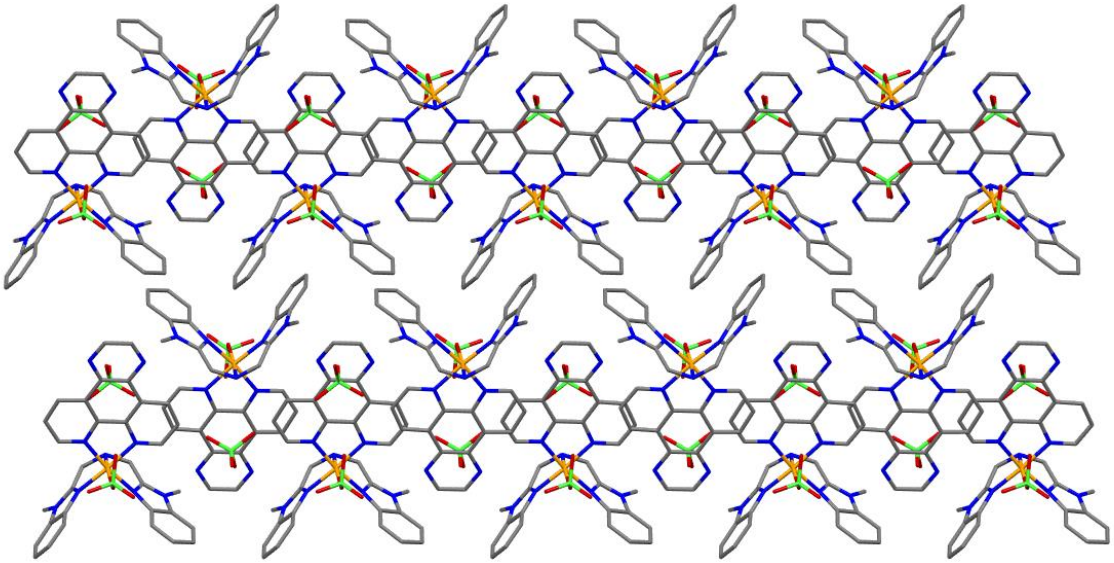

Fig. S22 Crystal packing of **4** viewed along the *a*-axis.

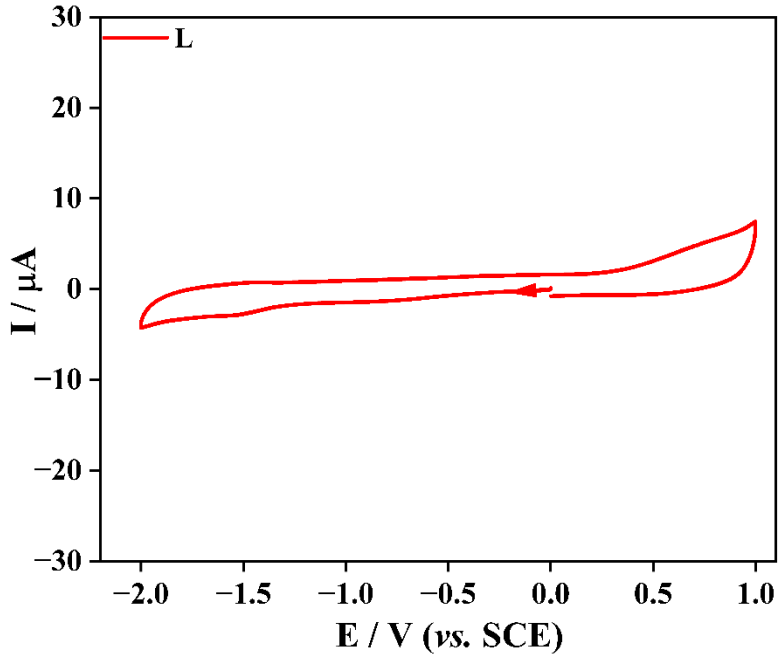

Fig. S23 CV of ligand **L** in dry DMF solvent using 0.1 M TBAP as supporting electrolyte under an inert atmosphere at a scan rate of 100 mV s^{-1}.

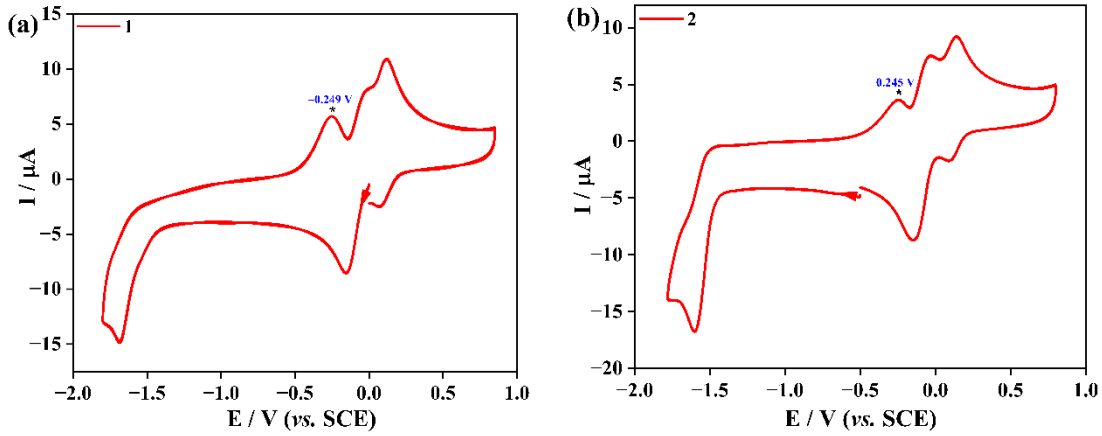

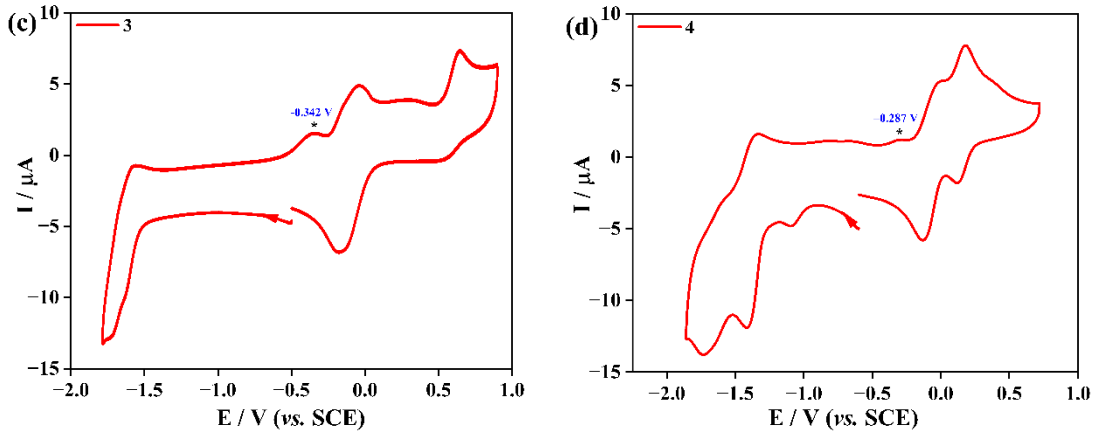

Fig. S24 CV of (a) **1**, (b) **2**, (c) **3**, and (d) **4** in dry DMF solvent using 0.1 M TBAP as supporting electrolyte under an inert atmosphere. The * peak indicates the copper deposition on the electrode surface, for $Cu^0 \rightarrow Cu^I$ oxidation.

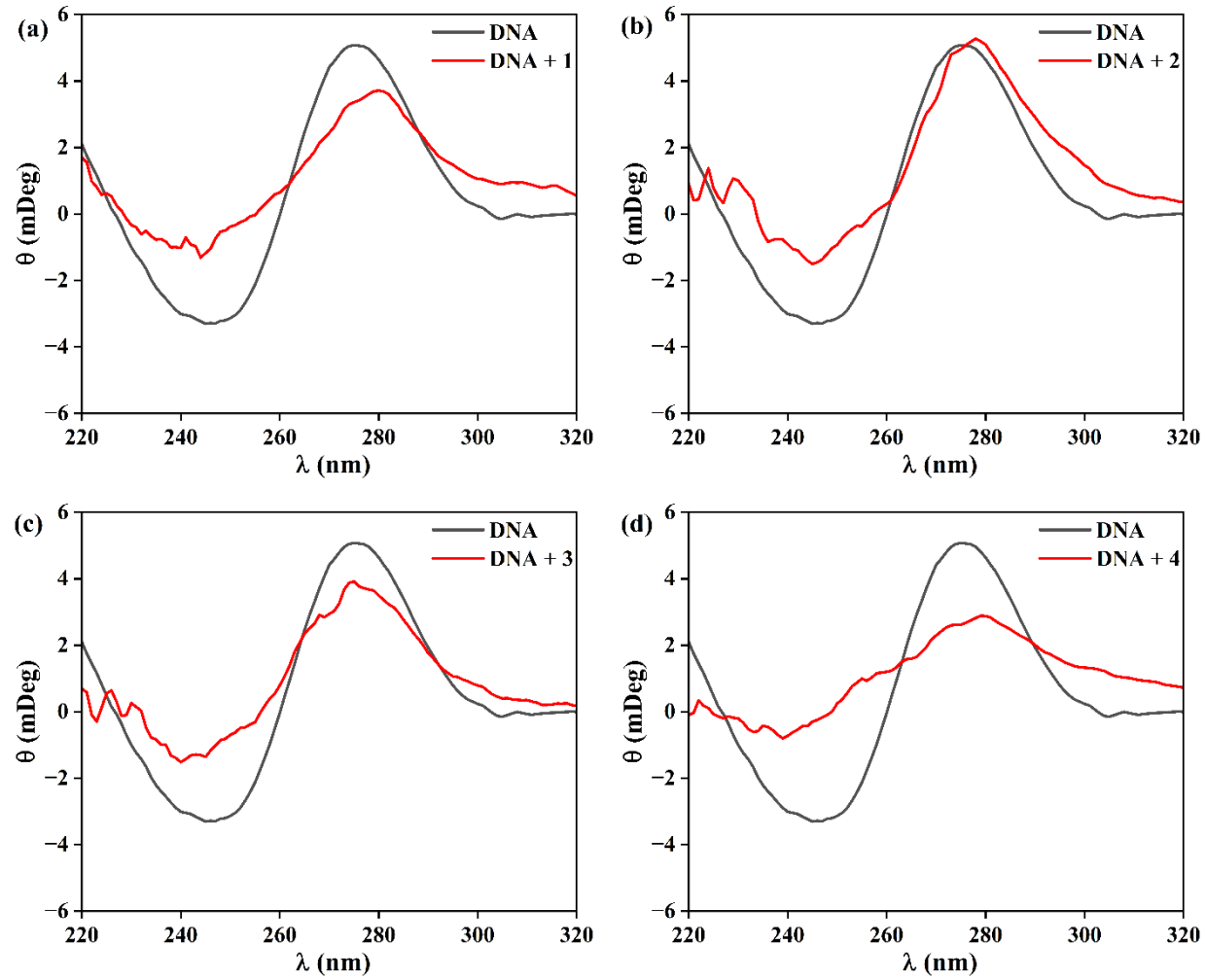

Fig. S25 CD spectra of ss-DNA (100 μM) in the absence (black line) and presence (red line) of (a) **1**, (b) **2**, (c) **3**, and (d) **4**.

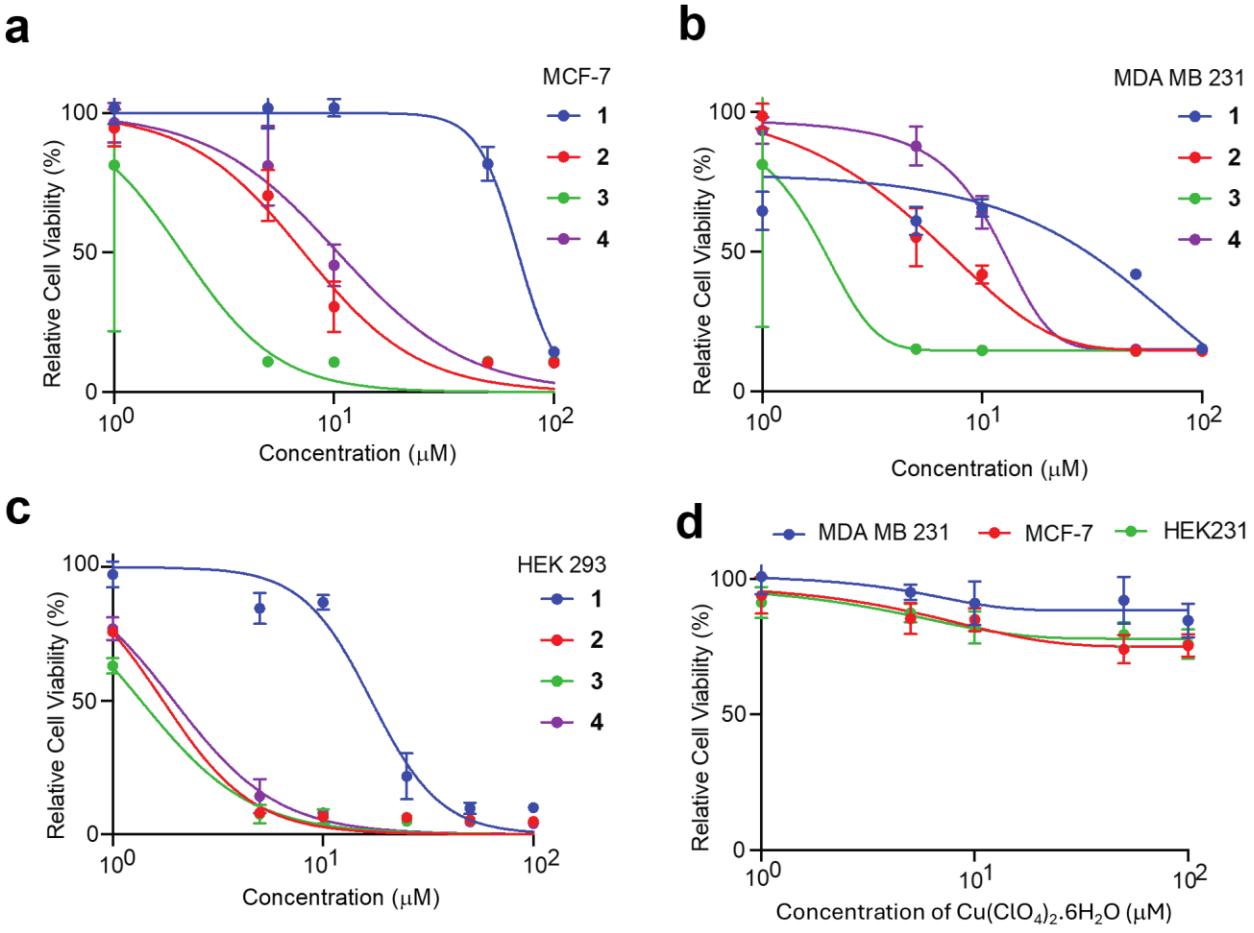

Fig. S26 Evaluation of cytotoxicity. (a-c) MTT assay evaluating the cytotoxic effects of **1**–**4**. MCF7, MDA-MB-231, and HEK293 cells were treated with each compound, and cell viability was assessed based on the reduction of MTT to formazan. (d) MTT assay evaluating the cytotoxic effects of $Cu(ClO_4)_2 \cdot 6H_2O$ in MCF7, MDA-MB-231, and HEK293 cells**.** Absorbance was measured at 570 nm, and results are expressed as mean ± SD from three independent experiments.